Royal College of Surgeons in Ireland

repository@rcsi.com

Validation of an imageable surgical resection animal model of Glioblastoma (GBM).

AUTHOR(S)

Kieron Sweeney, Monika A. Jarzabek, Patrick Dicker, Donncha O'Brien, John J. Callanan, Annette Byrne, Jochen Prehn

CITATION

Sweeney, Kieron; Jarzabek, Monika A.; Dicker, Patrick; O'Brien, Donncha; Callanan, John J.; Byrne, Annette; et al. (2014): Validation of an imageable surgical resection animal model of Glioblastoma (GBM).. Royal College of Surgeons in Ireland. Journal contribution. https://hdl.handle.net/10779/rcsi.10793255.v2

HANDLE

10779/rcsi.10793255.v2

LICENCE

CC BY-NC-SA 4.0

This work is made available under the above open licence by RCSI and has been printed from https://repository.rcsi.com. For more information please contact repository@rcsi.com

URL

https://repository.rcsi.com/articles/journal_contribution/Validation_of_an_imageable_surgical_resection_animal_model_of_Glioblastoma_GBM_/10793255/2

Validation of an imageable surgical resection animal model of Glioblastoma

Kieron J Sweeney [1,2,] Monika Jarzabek PhD [2], Patrick Dicker PhD[3], Donncha F O'Brien MD[1], Annette T. Byrne PhD[2]*, Jochen HM Prehn PhD[2]*

[1]National Centre for Neurosurgery, Beaumont Hospital, Dublin.

[2]Centre for Systems Medicine, Department of Physiology and Medical Physics, Royal College of Surgeons in Ireland, Dublin.

[3]Department of Epidemiology & Public Health Medicine, Royal College of Surgeons in Ireland, Dublin.

*Equal Contribution as Senior Authors

Corresponding Author: Kieron J. Sweeney

Phone: 00353 1 402 8512

Fax: 00353 1 402 8512

Email: kieron.sweeney@gmail.com

Key Words: GBM, surgical resection model, bioluminescence

Running Title: BLI surgical resection model of GBM with craniectomy repair.

A portion of this work was presented in abstract form at the Autumn meeting of the Society of British Neurological Surgeons on 26th September 2012.

Abstract

Glioblastoma (GBM) is the most common and malignant primary brain tumour with a median survival ranging between 12-18 months following standard therapy protocols. Local recurrence post-resection and adjuvant treatment occurs in most cases. Preclinical models exist which recapitulate the essential features of GBM. However, few have attempted to recapitulate the surgical resection environment and post-resection recurrence. Within the current context we have developed a robust methodology for establishing an imageable GBM surgical resection animal model.

Methods: 10^6 U87-MG luciferase expressing GBM cells were implanted into the right hemisphere of 6 week old female rats at predefined stereotactic co-ordinates (n=10). When tumour were in exponential growth phase (as measured from tumour emitting bioluminescence), animals were randomized into surgical and non-surgical groups. Following parenterally delivered anesthesia, animals were fixed in a stereotactic frame. A 4.5mm craniectomy was performed with resection of the tumour using microsurgical techniques. Hemostasis was ensured. The cranial defect was repaired using a novel modified cranial window technique consisting of a circular microscope coverslip held in place with glue.

Results:

Immediate post-operative bioluminescence imaging revealed a gross total resection rate of 75%. At censor point 4 weeks post-resection, Kaplan-Myer survival analysis revealed 100% survival in the surgical group compared to 0% in the non-surgical cohort (p=0.01). There were no neurological defects or infections in the surgical group. GBM recurrence was reliably imageable with a recurrence rate was observed by 4 weeks.

Conclusion:

We have established a reproducible, imageable surgical resection model of intracranial GBM that mimics patient recurrence post-resection.

Introduction

Glioblastoma (GBM) is the most frequent and malignant primary brain tumour which accounts for approximately 12-15% of all intracranial neoplasms [3]. GBM is heterogeneous on a genetic, cellular and macroscopic level. Intratumoural hypoxic gradients can drive stem cell distribution and effect epigenetic modifications such as MGMT expression. Current standard of care for GBM involves surgical resection followed by adjuvant chemo-radiotherapy. Extent of surgical resection can have the single greatest survival benefit for patients, with subtotal resections up to 78% providing a significant survival advantage [15]. It has also been demonstrated that surgery can improve the efficacy of adjuvant therapy [20]. Despite maximal treatment, GBM is characterized by tumour recurrence and resistance. Recurrence is due to tumour cell migration from the tumour bulk into normal surrounding brain parenchyma to where it is protected by an intact blood-brain-barrier. Resistance is due to complex intracellular and extracellular mechanisms. Genetic and epigenetic factors, tumour cell heterogeneity including the presence of stem cells, as well as the tumour microenvironment have all been implicated in resistance to treatment. The survival benefit conferred by surgery may derive from the concept of cytoreduction; by removing the bulk of the tumour and therefore its constituents implicated in resistance and recurrence, thereby improving the efficacy of adjuvant treatment [7,11,12,16,20,23]. Surgery also reduces the compressive biomechanical forces

of the tumour which can influence invasion and proliferation of GBM cells and pharmacodynamics of the drugs used[2,5,17-19,24].

Within the pre-clinical setting a majority of studies which employ GBM rodent models involve a non-surgical therapeutic regimen, and do not consider the therapeutic advantage of surgery which may significantly reduce the translational context. Herein, we describe the development of a novel cost effective imageable rat intracranial GBM surgical resection model. We describe a detailed protocol based on a novel modified cranial window technique to simultaneously repair the craniectomy and permit serial bioluminescence (BLI) imaging over a prolonged follow-up period.

Materials and Methods

Cell culture

U-87 MG-luc2 cells were sub-cultured in a T-75 flask. When the monolayer reached approximately 80 % confluence, the waste media was removed and the cells were washed with sterile Hanks Balanced Salt Solution (HBSS) (Sigma-Aldrich, St. Louis, MO, USA). Cells were then enzymatically detached from the surface of the tissue culture vessel following addition of 2 mls of a 0.25 % Trypsin-EDTA solution (Sigma-Aldrich, St. Louis, MO, USA). The flasks were returned into the incubator for 2-3 minutes and then struck once to ensure total cell detachment. The enzyme was inactivated by adding 5ml of volume of complete growth medium. The cell suspension was then transferred to a sterile centrifuge tube and spun at 1000 rpm for 3 min. The supernatant was removed and the resulting pellet was re-suspended in 10 ml of culture medium pre-warmed to 37°C and seeded at the 2.1×10^6 density in a T-75 culture flask. Cells were returned to the incubator and maintained at 37°C in humidified air with 5 % CO2.

Implantation of U87 MG- Luc 2 cells

10 Foxn1^{rnu} T-cell-deficient, athymic nude rats (Charles River Laboratories, Germany) were selected as they are suitable for glioblastoma tumour xenograft research [14]. The rats were weighed and anaesthetized via intraperitoneal delivery of anesthetic (ketamine (80mg/kg)/ xylazine 10mg/kg). Respiration was closely monitored along with the general condition of the animal. Skin was prepared by removing hair with a depilatory cream. The rats were then fixed in a stereotactic frame and the skin was disinfected with alcohol.

A small right parasagittal skin incision was made followed by a craniostomy with a high speed dental drill at the level of the bregma 3mm right of the midline. After the dura was punctured, 2µl of cell suspension containing 10^5 U87 MG-luc 2 cells were aspirated using a Hamilton syringe. The syringe was loaded into the stereotactic arm and cell suspension slowly injected at a depth of 2.5mm. The syringe was slowly withdrawn. Any residual cell suspension removed. The skin was closed in a single layer with 4/0 interrupted simple sutures. Animals were monitored post-operatively and returned to their cages when fully recovered. All animal experiments were licensed by the Department of Health and Children, Dublin, Ireland. Protocols were reviewed by the Royal College of Surgeons in Ireland (RCSI) Animal Research Ethics Committee (AREC).

Bioluminescence imaging (BLI)

D-Luciferin [d-(-)-2-(60-hydroxy-20-benzothiazolyl)-thiazone-4-carboxylic acid] (Caliper Life Sciences, USA) was formulated in a 30mg/ml solution of DPBS without calcium and magnesium, filtered through a 0.22 µm filter, and protected from light. A kinetic study was performed at week 1 and 2 post implantation to generate a kinetic curve of luciferase activity. Images were analyzed with Living Image® Software (PerkinElmer Inc.) using fixed regions of

interest. Animals were imaged in identical fashion each week using peak signal time established by the week 2 kinetic study.

Surgical resection

When tumors were in exponential growth phase as determined by bioluminescence signal, the animals were randomized into 2 groups: Control/Non-surgical group and surgical group. Rats were weighed and intraperitoneal delivery of anesthetic [ketamine (80mg/kg)/ xylazine 10mg/kg]. No antibiotics were administered for the experiment. Animal respiration and general condition were closely monitored. The skin was prepared by removing hair with a depilatory cream. The rats were then fixed in a stereotactic frame and the skin was prepared in standard surgical fashion.

Previous skin incision was extended in a curvilinear fashion and tissues reflected back. The temporalis muscle was sharply dissected from the cranium and reflected and the pericranium incised and also reflected. The previous burr hole was identified. Using an operating microscope and high-speed dental drill a 4.5mm craniectomy was made centered on the previous burr hole. A durotomy was made and the tumour located. The tumour was gently dissected free (see figure 1). Hemostasis was achieved with a hand-held electrocautery pen with a fine needle tip. The surgical cavity was irrigated and filled with sterile saline.

To repair the cranial defect and to permit post-operative BLI, 5mm sterile circular glass microscope coverslips were placed and fixed with cyanoacrylate glue (see figure 1). The skin was closed in a single layer over the cranial window with 4/0 interrupted simple sutures and cleaned with alcohol (see figure 1). Animals underwent immediate post-operative BLI and were returned to their cage when fully recovered (see figure 2). Animals were weighed daily

and assessed for wound infection and general condition. Neurological function was assessed by a previously described method using a modified rat coma scale[1].

Statistical Analysis

Kaplan-Meier survival analysis and graphs were collated using GraphPad Prism 5 ®.

Results

Bioluminescence signal as a marker of pre-operative tumour growth

We performed bioluminescence imaging of animals at weekly intervals to assess tumour growth. Total photon flux was plotted each week. From this we established that all tumors were in the exponential growth phase by week 4.5. (see figure 3). At this time point the animals were randomized into surgical and non-surgical/control groups.

Bioluminescence signal to establish extent of resection and tumour recurrence.

Those animals undergoing surgical resection had bioluminescence imaging immediately pre-operatively and post-operatively (see figure 3). From this we established that we had achieved a gross total resection rate of 75%. In one single rat we were able to detect tumour signal quantified at 7.58×10^4 photons/sec/cm^2. Although this was below background threshold levels, we consider this to be a sub-total resection as it was two-times the total flux of the other surgical resection animals (mean 3.06×10^4 photons/sec/cm^2. Post-operative bioluminescence imaging analysis reveals that we achieved greater than 99% reduction in total photon flux.

Each post-operative week the animals were imaged in identical fashion and the total photon flux plotted. There was a stepwise incidence of tumour recurrence as noted by bioluminescence signal beginning with the rat that had the sub-total resection. By the fourth

post-operative week the mean signal of the operative group exceeded the pre-operative mean total photon flux ($1.83x10^8$ v $2.61x10^8$ photons/sec/cm^2) (see figure 4 & 5).

Surgical resection of the intracranial tumour increases survival.

All surgical animals survived to the end of the study period. Censor point was at 4 weeks to facilitate further histological analyses. In the surgical group, weights and general condition were consistent throughout the study period. Kaplan-Meier Survival analysis revealed surgery conferred a statistically significant survival advantage (Log-Rank p=0.01) (see figure 6)

Histology

Post mortem histological analysis revealed a marked unilateral tumour causing mass effect in the superficial cortex of the non-surgical/control animals. These tumors display patchy areas of necrosis surrounded by areas of pseudopallisading. There was marked neovascularization with minimal invasion into the surrounding normal brain parenchyma (see figure 7 & 8). In animals that underwent surgery, the resection cavity was apparent and both histological examination and ex-vivo BLI signal confirmed tumour in this cavity. (see figure 9).

Discussion

To date a limited number of studies have utilized any form of intracranial surgical resection in pre-clinical GBM models [1,4,25]. These studies have relied only on survival analysis and histology to interpret the efficacy of intracavity chemotherapeutics. Moreover, such resection models ostensibly lack any attempt to longitudinally assess treatment response via molecular imaging. Thus, to extend and improve upon efforts to date we have developed a novel rat

based xenograft model wherein bioluminescence imaging combined with a modified cranial window technique facilitates serial imaging follow-up.

To our knowledge, just two studies have utilized a BLI surgical resection model of GBM. The first investigated encapsulated stem cell migration in combination with intravital microscopy [8]. In this paper the authors successfully used a "cranial window" to perform surgical resection and deliver encapsulated stem cells. The "cranial window" as described consisted of craniectomy only, with direct wound closure. In the second surgical resection paper that employed BLI, the authors also did not repair the cranial defect[6]. The limitation of this approach is that the surgical resection cavity is in direct continuation with the subgaleal space which may preclude this model from being used in the development of intracavity delivery of novel non-biological agents, particularly cytotoxic agents. Within the clinical context (based on the author's observations) use of carmustine wafers elicits a higher incidence of wound complications when the dura is not closed in a watertight fashion. Thus, herein we have described a detailed step-by-step procedure for performing intracranial surgical resection and cranial defect repair, which separates the surgical cavity from the overlying tissues and enables facile non-invasive bioluminescence imaging follow-up.

Hallmarks of the natural history of GBM, despite maximal standard therapy are recurrence and resistance, or poor response to re-treatment and second line/salvage therapy. It is clear that extent of tumour resection is an important determinant of survival and it has been suggested that it may also improve the efficacy of adjuvant treatment [20,21]. In the current context we have successfully recapitulated the clinical GBM resection strategy. Our data closely correlates with observations from clinical practice. We achieved a gross total resection rate of 75% with a 75% recurrence rate at four weeks. Clinically, depending on the neurosurgical centre and the methods employed to maximize surgical resection, gross total resection rates have been reported in the 65%-94% range [9,10,22]. We have also demonstrated a survival benefit due to surgery alone as noted by a week 4 censored Kaplan-Meier analysis ($p=0.01$). This also reflects clinically observed survival benefits. Previous studies have shown that pa-

tients who undergo biopsy only, have poorer survival rates than those who have had a surgical resection [13].

Perhaps the most important finding in our current study is the ability to image tumour recurrence post-surgical resection. Application of a surgical resection rat model (as distinct from mouse) in pre-clinical GBM therapeutic efficacy studies may better facilitate: (1) the study of combinatorial and sub-chronic/chronic dosing regimens due to practical benefits associated with larger rodents (e.g. ability to more easily perform repeated oral/ intravenous dosing procedure), (2) may facilitate improved application of state of the art translational molecular imaging strategies with specific application in the study of GBM (e.g. CT and functional MRI), and (3) may also better integrate with rodent toxicology (rat) studies generally required for regulatory approval of novel targeted therapies/ combinatorial treatment strategies.

Conclusion

We have established an imageable surgical resection rat model of GBM. This model will account for the therapeutic benefit of surgical resection in pre-clinical models.This model may also account for one of the main reasons of treatment failure, residual tumour protected by an intact BBB.

Disclosure:

The authors report no conflicts of interest.

Acknowledgements

This research was supported by a grant from Science Foundation Ireland (08/IN1/B1949) and by the National Biophotonics and Imaging Platform Ireland (PRTLI Cycle 4) funded through the Irish Higher Education Authority. Dr Annette Byrne receives funding in the context of the EU Framework Programme 7 'AngioTox' (www.angiotox.com) and 'Angiopredict' (www.angiopredict.com).

1. Akbar U, Jones T, Winestone J, Michael M, Shukla A, Sun Y, et al: Delivery of temozolomide to the tumor bed via biodegradable gel matrices in a novel model of intracranial glioma with resection. **Journal of Neuro-Oncology 94:**203-212, 2009
2. Boucher Y, Salehi H, Witwer B, Harsh GRt, Jain RK: Interstitial fluid pressure in intracranial tumours in patients and in rodents. **Br J Cancer 75:**829-836, 1997
3. David N. Louis HO, Otmar D. Wiestler, Webster K. Cavenee. (ed): **The WHO Classification of Tumours of the Central Nervous System, ed 4th.** Lyon: IARC, 2007
4. Emerich DF, Winn SR, Hu Y, Marsh J, Snodgrass P, LaFreniere D, et al: Injectable chemotherapeutic microspheres and glioma I: enhanced survival following implantation into the cavity wall of debulked tumors. **Pharm Res 17:**767-775, 2000
5. Heldin C-H, Rubin K, Pietras K, Östman A: High interstitial fluid pressure — an obstacle in cancer therapy. **Nature Reviews Cancer 4:**806-813, 2004
6. Hingtgen S, Figueiredo JL, Farrar C, Duebgen M, Martinez-Quintanilla J, Bhere D, et al: Real-time multi-modality imaging of glioblastoma tumor resection and recurrence. **J Neurooncol 111:**153-161, 2013
7. Jamal M, Rath BH, Tsang PS, Camphausen K, Tofilon PJ: The brain microenvironment preferentially enhances the radioresistance of CD133(+) glioblastoma stem-like cells. **Neoplasia 14:**150-158, 2012
8. Kauer TM, Figueiredo J-L, Hingtgen S, Shah K: Encapsulated therapeutic stem cells implanted in the tumor resection cavity induce cell death in gliomas. **Nature Neuroscience 15:**197-204, 2011
9. Kubben PL, ter Meulen KJ, Schijns OE, ter Laak-Poort MP, van Overbeeke JJ, van Santbrink H: Intraoperative MRI-guided resection of glioblastoma multiforme: a systematic review. **Lancet Oncol 12:**1062-1070, 2011
10. Lenaburg HJ, Inkabi KE, Vitaz TW: The use of intraoperative MRI for the treatment of glioblastoma multiforme. **Technol Cancer Res Treat 8:**159-162, 2009
11. Mannino M, Chalmers AJ: Radioresistance of glioma stem cells: Intrinsic characteristic or property of the 'microenvironment-stem cell unit'? **Molecular Oncology 5:**374-386, 2011
12. Ng WH, Wan GQ, Too HP: Higher glioblastoma tumour burden reduces efficacy of chemotherapeutic agents: in vitro evidence. **Journal of Clinical Neuroscience 14:**261-266, 2007
13. Patwardhan RV, Shorter C, Willis BK, Reddy P, Smith D, Caldito GC, et al: Survival trends in elderly patients with glioblastoma multiforme: resective surgery, radiation, and chemotherapy. **Surg Neurol 62:**207-213; discussion 214-205, 2004
14. Rubenstein JL, Kim J, Ozawa T, Zhang M, Westphal M, Deen DF, et al: Anti-VEGF antibody treatment of glioblastoma prolongs survival but results in increased vascular cooption. **Neoplasia 2:**306-314, 2000

15. Sanai N, Polley M-Y, McDermott MW, Parsa AT, Berger MS: An extent of resection threshold for newly diagnosed glioblastomas. **Journal of Neurosurgery 115:**3-8, 2011
16. Shi L: MicroRNA-125b-2 confers human glioblastoma stem cells resistance to temozolomide through the mitochondrial pathway of apoptosis. **International Journal of Oncology**, 2011
17. Shieh AC: Biomechanical Forces Shape the Tumor Microenvironment. **Annals of Biomedical Engineering 39:**1379-1389, 2011
18. Shieh AC, Rozansky HA, Hinz B, Swartz MA: Tumor Cell Invasion Is Promoted by Interstitial Flow-Induced Matrix Priming by Stromal Fibroblasts. **Cancer Research 71:**790-800, 2011
19. Shieh AC, Swartz MA: Regulation of tumor invasion by interstitial fluid flow. **Physical Biology 8:**015012, 2011
20. Stummer W, Bent MJ, Westphal M: Cytoreductive surgery of glioblastoma as the key to successful adjuvant therapies: new arguments in an old discussion. **Acta Neurochirurgica 153:**1211-1218, 2011
21. Stummer W, Meinel T, Ewelt C, Martus P, Jakobs O, Felsberg J, et al: Prospective cohort study of radiotherapy with concomitant and adjuvant temozolomide chemotherapy for glioblastoma patients with no or minimal residual enhancing tumor load after surgery. **Journal of Neuro-Oncology 108:**89-97, 2012
22. Stummer W, Pichlmeier U, Meinel T, Wiestler OD, Zanella F, Reulen H-J: Fluorescence-guided surgery with 5-aminolevulinic acid for resection of malignant glioma: a randomised controlled multicentre phase III trial. **The Lancet Oncology 7:**392-401, 2006
23. Tanaka K, Babic I, Nathanson D, Akhavan D, Guo D, Gini B, et al: Oncogenic EGFR Signaling Activates an mTORC2-NF- B Pathway That Promotes Chemotherapy Resistance. **Cancer Discovery 1:**524-538, 2011
24. Tse JM, Cheng G, Tyrrell JA, Wilcox-Adelman SA, Boucher Y, Jain RK, et al: Mechanical compression drives cancer cells toward invasive phenotype. **Proc Natl Acad Sci U S A 109:**911-916, 2012
25. Zhang X, Jiang F, Kalkanis SN, Yang H, Zhang Z, Katakowski M, et al: Combination of surgical resection and photodynamic therapy of 9L gliosarcoma in the nude rat. **Photochem Photobiol 82:**1704-1711, 2006

Figure 1-Detailed step-by-step description of surgical resection procedure. (i) 4.5 mm Craniectomy is fashioned with a high speed drill. Note the tumour presents itself into the craniectomy defect. (ii) Once the tumour is resected the surgical resection cavity is available to receive intracavity delivery of therapeutic agents. (iii) The modified cranial window technique that facilities the repair of the cranial defect allowing separation of the surgical resection cavity from the overlying tissues and simultaneously allowing bioluminescence imaging. The cranial window consists of a circular microscope coverslip help in situ with cyanoacrylate glue. Magnification 1x (iv) Closer view of the modified cranial window at a magnification of 3x demonstrating an air fluid level within the contained surgical resection cavity. (iv) After the cranial defect is repaired the wound is closed with simple interrupted absorbable sutures.

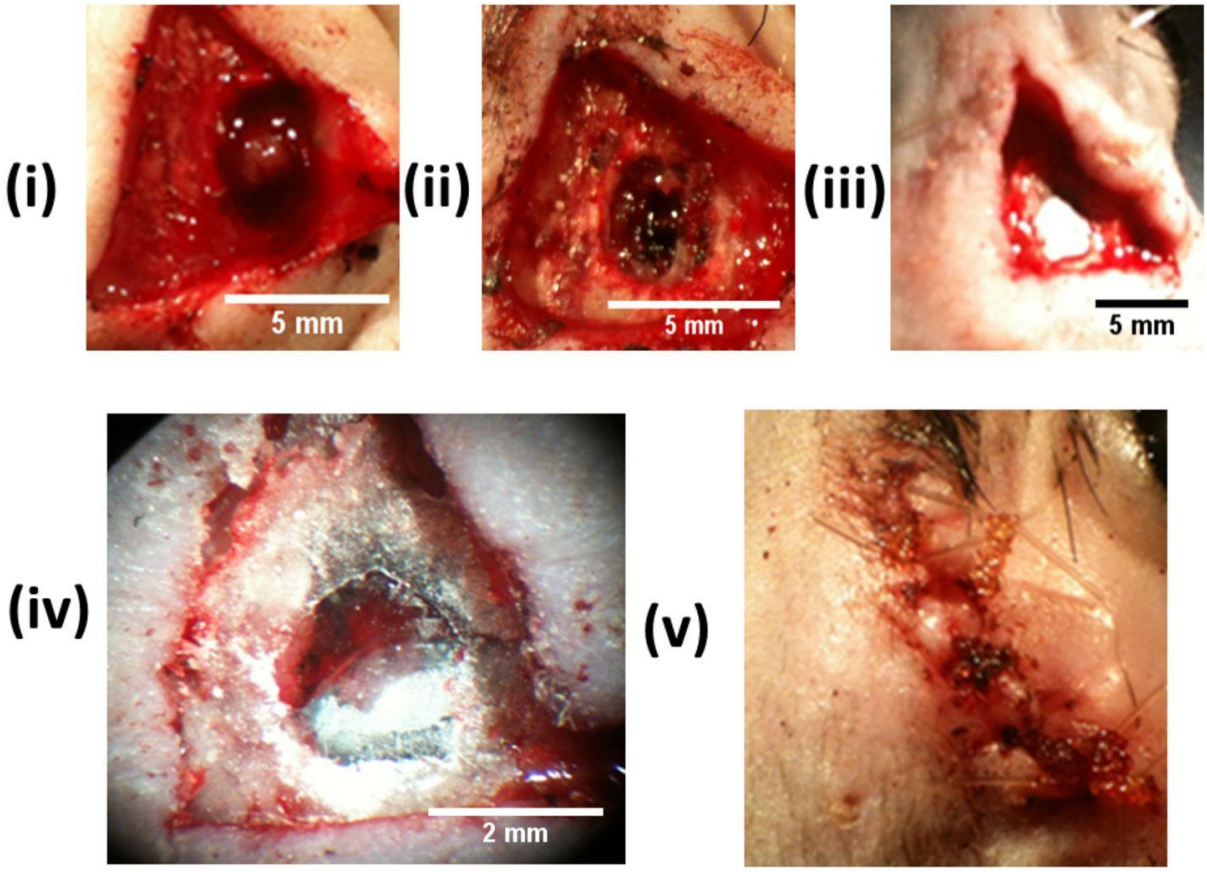

Figure 2- The Immediate post-operative Bioluminescence (BLI) imaging of the four animals that underwent surgical resection to establish the extent of resection. Note in all four animals (i)-(iv) there is a sharp reduction in the BLI signal. In (ii) the BLI signal over the surgical resection cavity was twice that of the others but remained below acceptable levels.

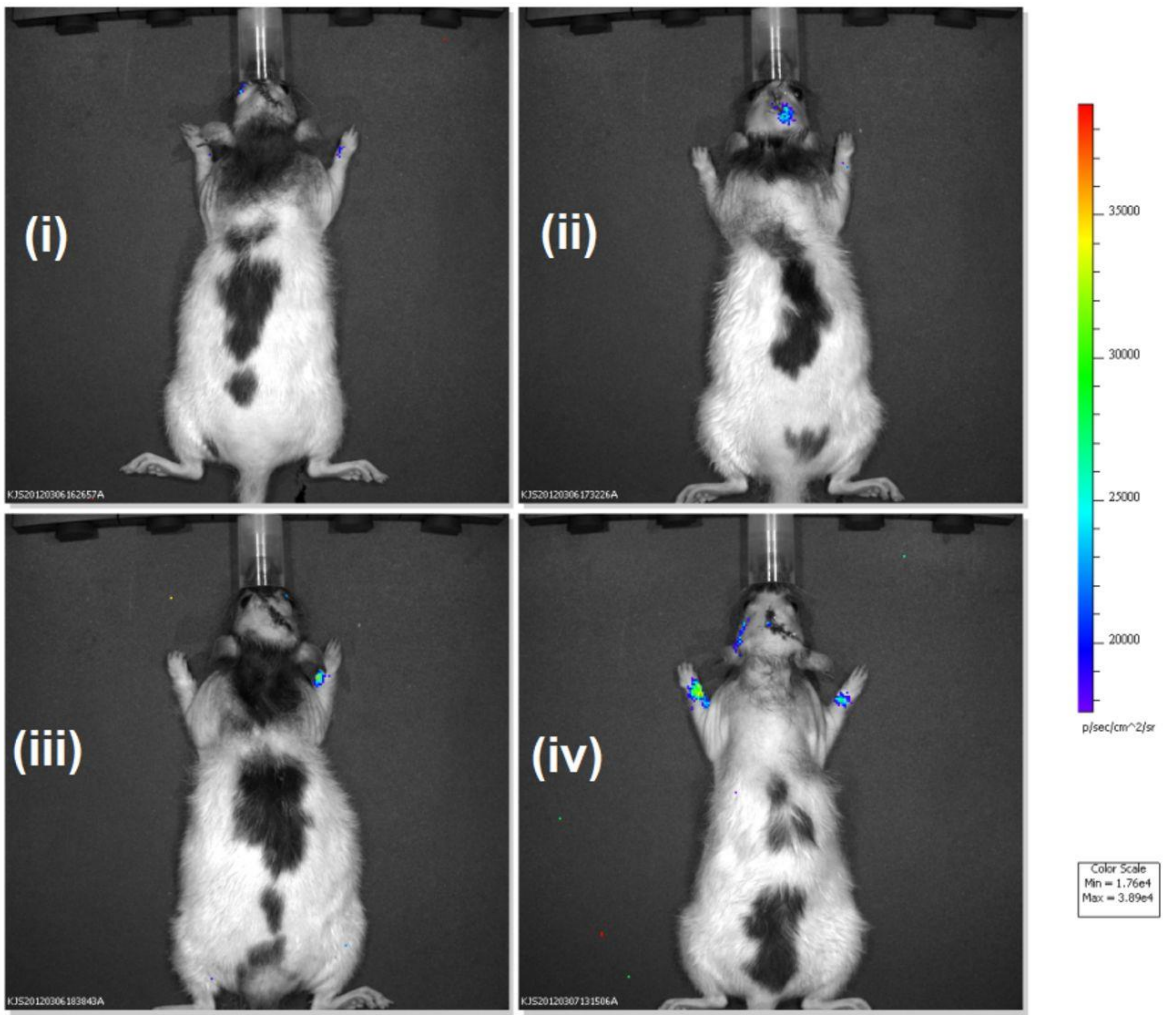

Figure 3- Longitudinal Bioluminescence (BLI) imaging of tumour growth after implantation and before surgical resection demonstrating the growth curve of the tumors before the animals were randomized into surgical and non-surgical groups. Whiskers represent SEM.

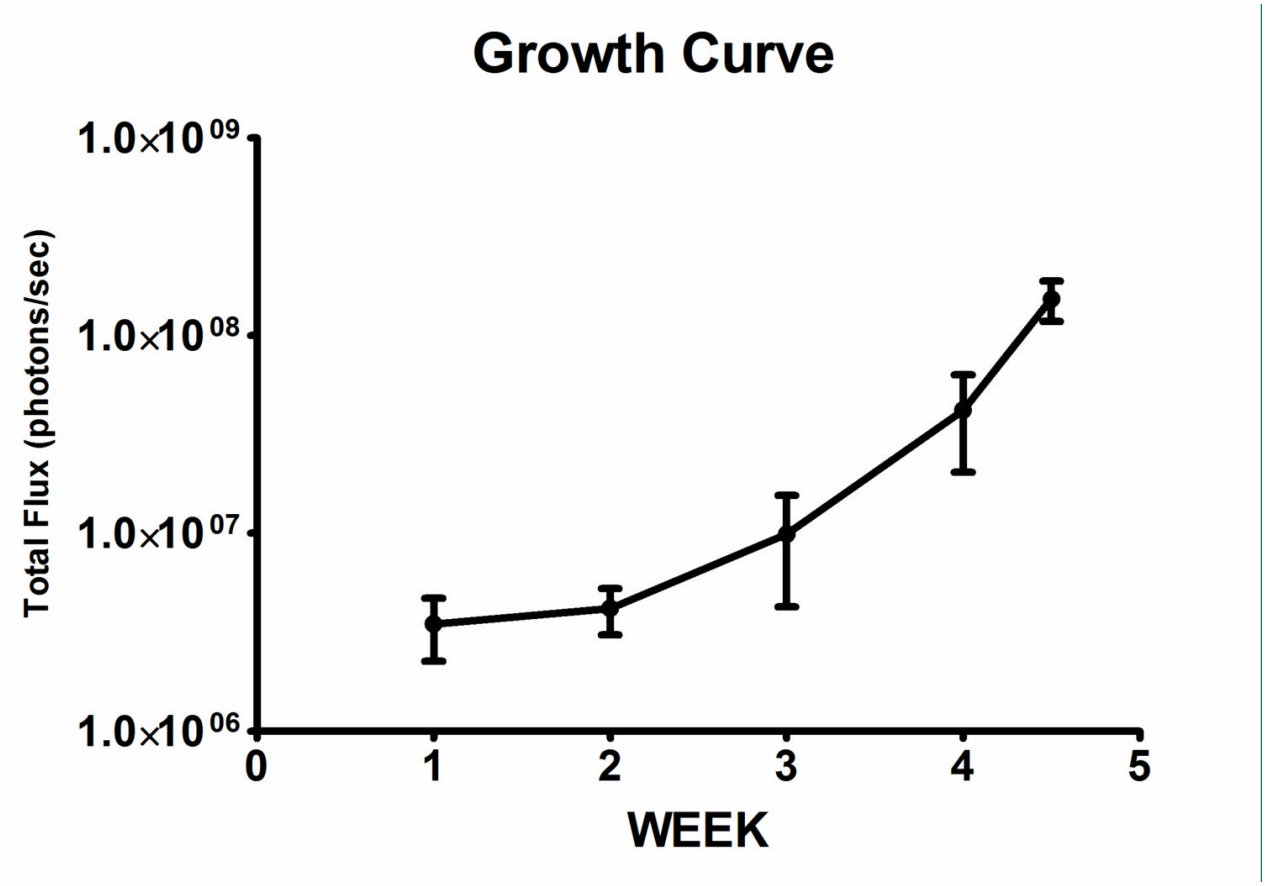

Figure 4- Longitudinal Bioluminescence (BLI) imaging of tumour growth of surgical group (grey) and non-surgical (black) groups. The sharp drop in the surgical group represents the time of surgical resection. Note the ability to longitudinally follow tumour recurrence in vivo after the cranial defect is repaired. Whiskers represent SEM.

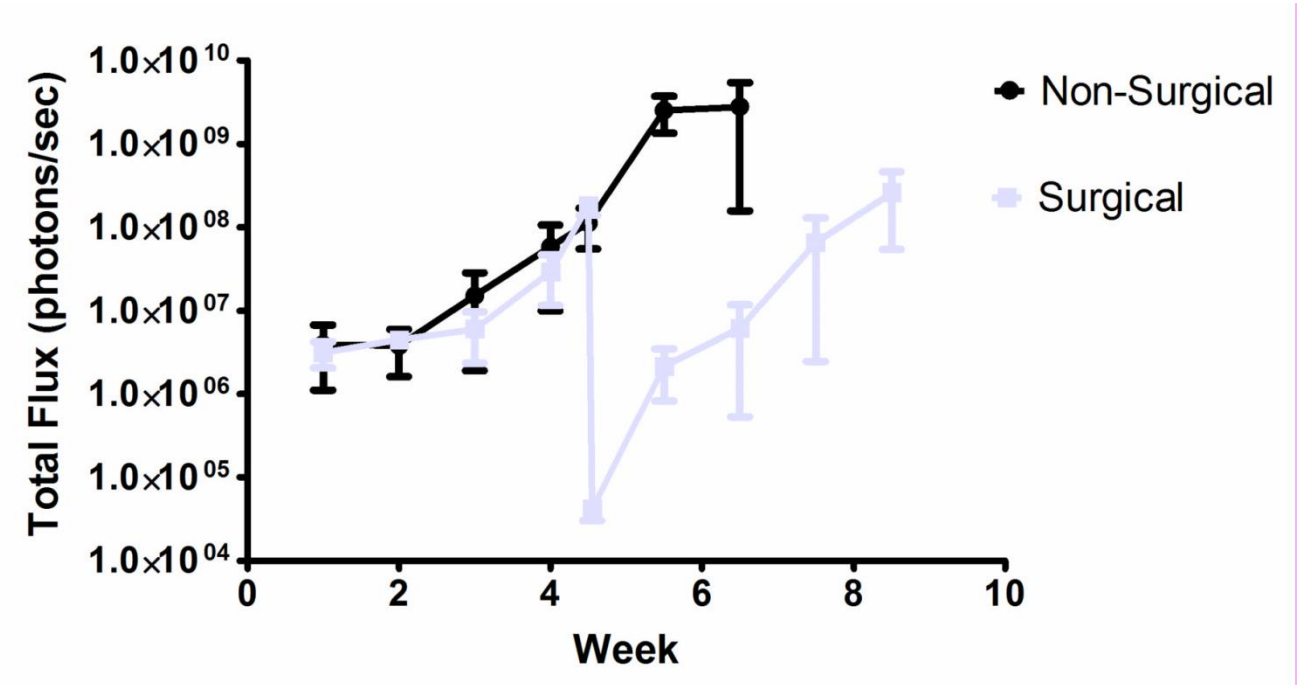

Figure 5- Representative longitudinal Bioluminescence (BLI) images from (i) surgical and (ii) non-surgical groups with corresponding ex-vivo images. Note in the surgical group the obvious drop in BLI in immediate post-operative image and the facile method of longitudinally imaging tumor recurrence.

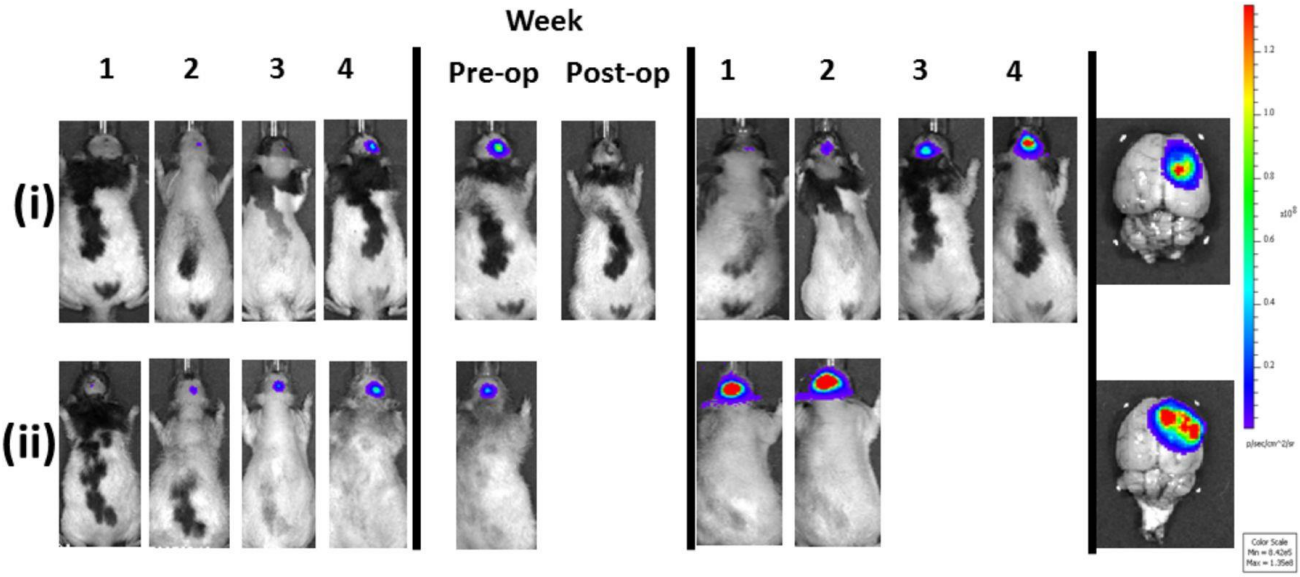

Figure 6- Kaplan-Meier survival curves of the surgical and non-surgical groups. Surgical resection of the tumors conferred a significant survival benefit group when compared to the control group. P<0.05.

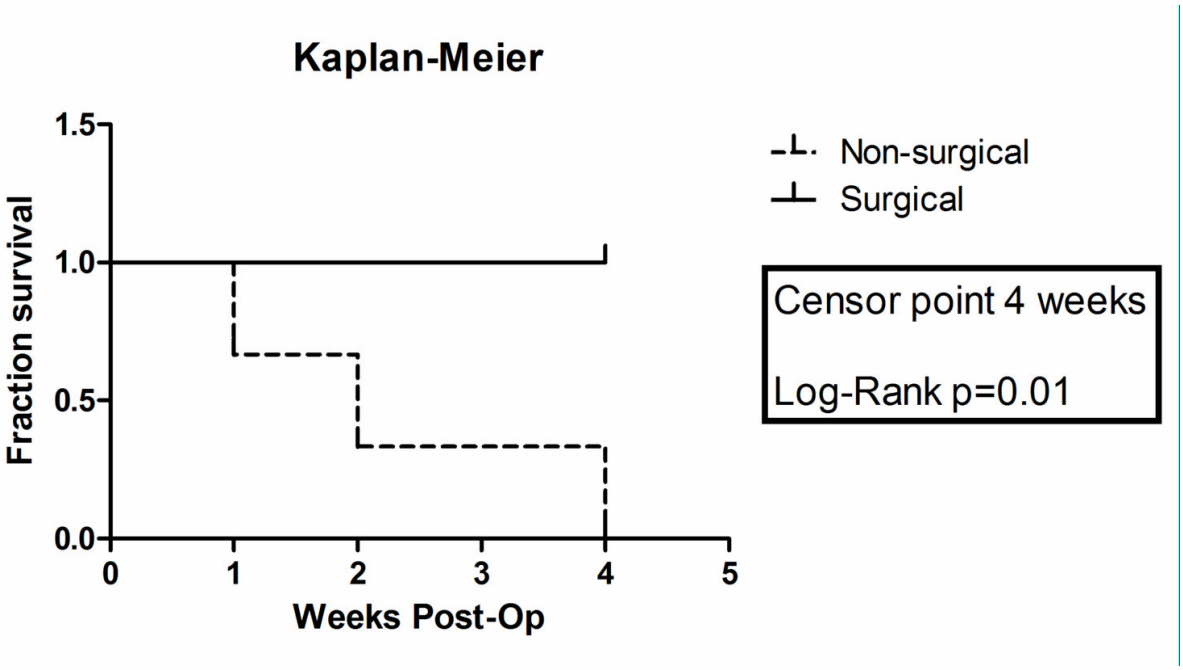

Figure 7- Low magnification micrograph in the coronal plane of non-surgical group using H&E staining demonstrating a dense cellular Glioblastoma U87-MG tumour in the subcortical area indicated by the white arrow. Magnification 20x

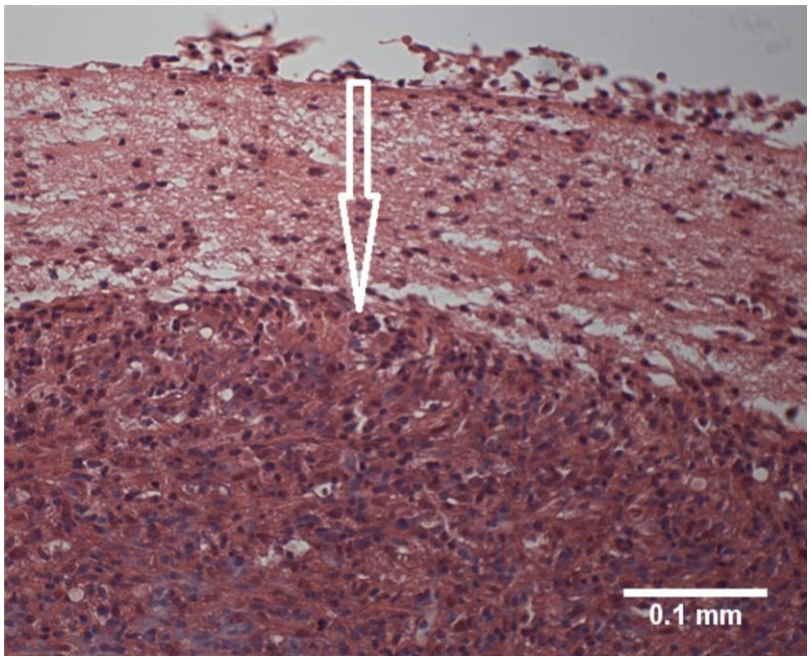

Figure 8- Higher magnification micrograph image of figure 35. Magnification 40x. White arrow indicates the dense cellular subcortical GBM.

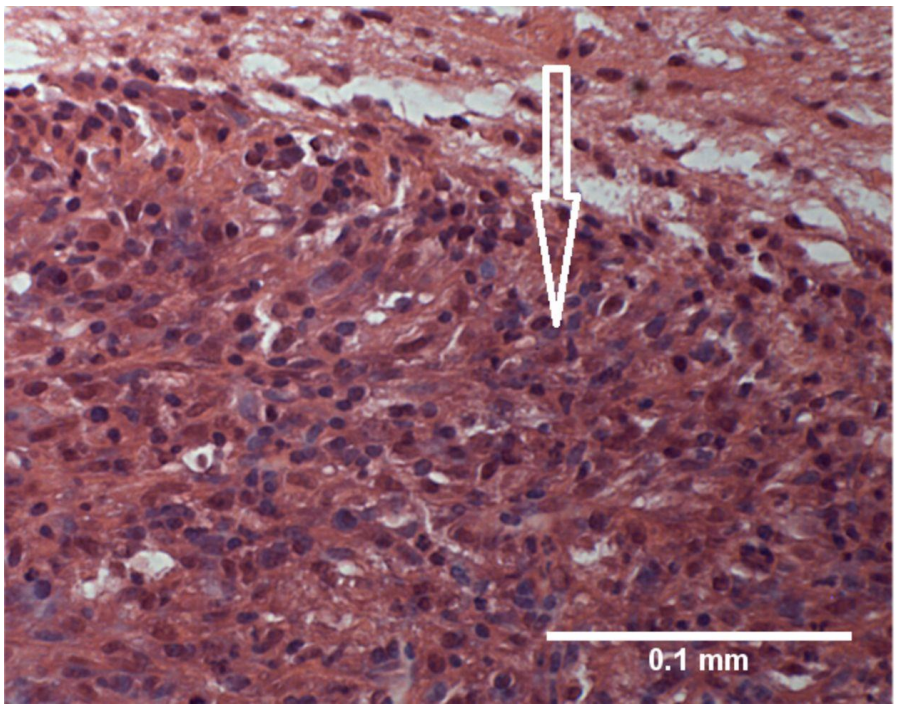

Figure 9- Low magnification micrograph image of the surgical resection cavity demonstrating residual tumour that has infiltrated the surgical resection cavity leading to tumour recurrence

which, using this model, we are able to image longitudinally in vivo. Residual tumor is indicated with arrows. H&E staining. Magnification 4x.